Quantitative modeling of the role of surface traps in CdSe/CdS/ZnS nanocrystal photoluminescence decay dynamics

Marcus Jones, Shun S. Lo, and Gregory D. Scholes[1]

Department of Chemistry, 80 Saint George Street, Institute for Optical Sciences, and Center for Quantum Information and Quantum Control, University of Toronto, Toronto, ON, Canada M5S 3H6

Edited by Michael L. Steigerwald, Columbia University, New York, NY, and accepted by the Editorial Board January 12, 2009 (received for review September 17, 2008)

Charge carrier trapping is an important phenomenon in nanocrystal (NC) decay dynamics because it reduces photoluminescence (PL) quantum efficiencies and obscures efforts to understand the interaction of NC excitons with their surroundings. Particularly crucial to our understanding of excitation dynamics in, e.g., multiNC assemblies, would be a way of differentiating between processes involving trap states and those that do not. Direct optical measurement of NC trap state processes is not usually possible because they have negligible transition dipole moments; however, they are known to indirectly affect exciton photoluminescence. Here, we develop a framework, based on Marcus electron transfer theory, to determine NC trap state dynamics from time-resolved NC exciton PL measurements. Our results demonstrate the sensitivity of PL to interfacial dynamics, indicating that the technique can be used as an indirect but effective probe of trap distribution changes. We anticipate that this study represents a step toward understanding how excitons in nanocrystals interact with their surroundings: a quality that must be optimized for their efficient application in photovoltaics, photodetectors, or chemical sensors.

quantum dot | states | electron transfer | time-correlated single-photon counting | fluorescence intermittency

Colloidal semiconductor nanocrystals (NCs) are potentially useful in a variety of photoactive applications because of their widely tunable electronic band gaps and their ease of processability. Different from well-studied molecular fluorophores, the excited electronic states of NCs with diameters in the range 1 to 10 nm are examples of nanoscale excitons (1). To be used in solar photovoltaics, for example, photo-generated NC excitons must be able to dissociate and transfer charge carriers to their surroundings in a controlled fashion; however, this process is impeded in NCs by the considerable influence of surface-localized states that trap carriers (2). Perturbations due to traps are important because of the significant surface-to-volume ratios characteristic of small colloids (3, 4). Certain surface sites act as charge acceptors that dissociate excitons and therefore reduce the photoluminescence (PL) quantum yield. Changes in solvent or surface-bound coordinating ligands have been found to affect these surface traps and thereby influence steady-state (5–9) and time-resolved (10–12) NC PL. The ability of surface traps to act as charge acceptors makes them excellent model systems for elucidating exciton dissociation processes occurring on the NC surface. Properties intrinsic to NC excitons have been examined in detail (13–17) but comparatively little is understood about the interplay among intrinsic excitons and surface states. Here, we report investigations of CdSe/CdS/ZnS core/shell/shell NC ensemble PL and establish a quantitative model of interfacial trapping and its effect on NC PL dynamics.

Colloidal CdSe NCs are coated with passivating ligands that sustain their dispersion in solution and minimize the number of surface atoms with reduced coordination number. Magnetic resonance studies (18–23) have probed the nature of NC-ligand-binding interactions and it is typically found (24, 25) that surface coverage is incomplete. Unbound surface atoms constitute a distribution of localized sites that carry slight positive or negative charge after local distortions minimize surface free energy (26). These sites are capable of trapping electrons or holes at the surface. Ab initio calculations (27) and positron annihilation spectroscopy on CdSe NCs (24) suggest that Se atoms relax outward irrespective of passivation, indicating, as previously suggested (25, 28–30), that hole traps constitute the majority surface trap site. The precise number of trap sites around a NC is likely to be both inhomogeneous and sample dependent; although consideration of the number of atoms near the surface in a wurtzite NC puts an approximate upper limit on that number (25). Some trap sites are also likely to exist between epitaxial layers in core–shell structures. Therefore, we have a satisfactory atomic-scale picture of the origins of surface traps, but what is presently lacking is a model that explains their role in NC photophysics.

NC trap states are typically dark, which means that their presence can only be inferred indirectly from PL signals. Nonetheless, there are 2 major advantages of using PL to examine trap states: (*i*) the well documented (5–12) sensitivity of NC PL to interface and environmental changes and (*ii*) the ability of time-resolved PL measurements to resolve processes that occur over a large dynamic range of timescales. Several groups (11, 31–37) have studied the influence of trap states on PL transients in CdSe NCs, and stochastic models have been used in some of these studies to extract radiative decay rates or trapping rates. Although such models successfully reproduce exciton-only dynamics, they have been unable to capture satisfactorily the influence of interface states. By elucidating such details we will be able to complete the picture of NC PL dynamics in terms of exciton and trap state populations.

Photoluminescence is perhaps the dominant technique for NC characterization, yet the processes that shape these PL dynamics are complex. Therefore, time-resolved NC PL is typically multiexponential and often endures for tens or hundreds of times longer than the ≈20-ns lifetime of the optically active exciton states from which PL arises (10–12, 38). Although a "dark" exciton state with a PL lifetime of ≈1 μs (39) is situated <20 meV below the bright exciton in wurtzite CdSe NCs, Boltzmann statistics ensure that this state cannot account for the long PL decay tails at room temperature. Instead, it is considered that PL decays indicate participation in the relaxation process of surface-related trap states. It is reasonable to imagine that these trap states would be members of a distribution in the ensemble, and are nonluminescent states whose population lifetimes span nanosecond to millisecond timescales.

Author contributions: M.J. and G.D.S. designed research; M.J. and S.S.L. performed research; M.J. analyzed data; and M.J. and G.D.S. wrote the paper.

The authors declare no conflict of interest.

This article is a PNAS Direct Submission. M.L.S. is a guest editor invited by the Editorial Board.

[1]To whom correspondence should be addressed. E-mail: gscholes@chem.utoronto.ca.

This article contains supporting information online at www.pnas.org/cgi/content/full/0809316106/DCSupplemental.

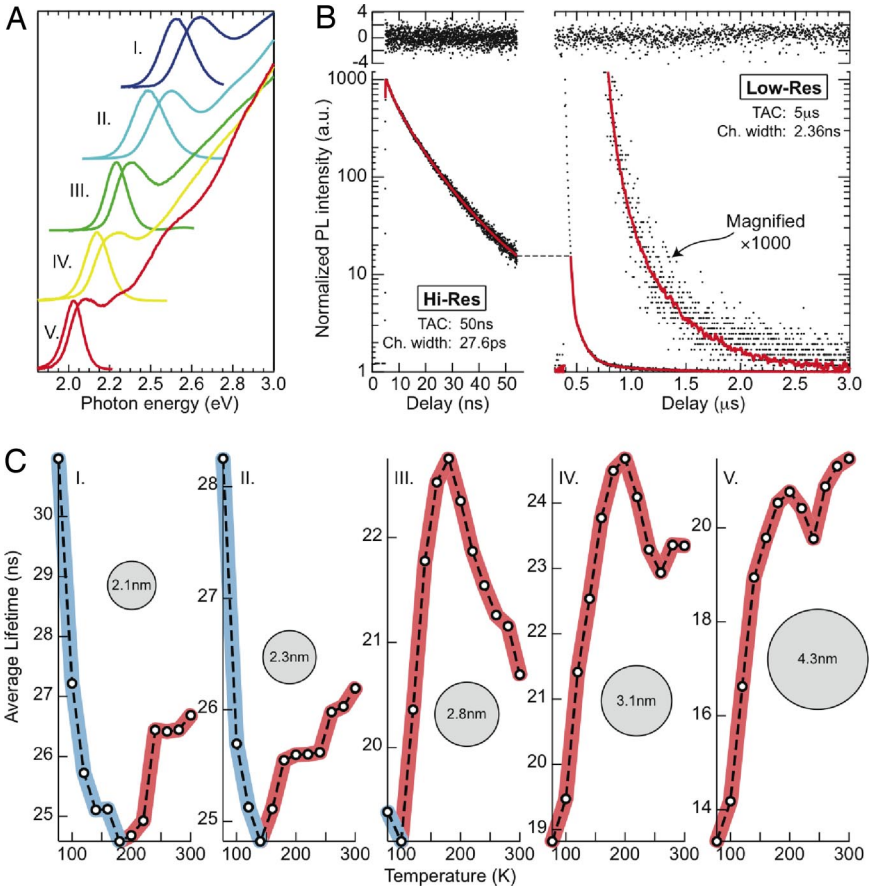

Fig. 1. Spectroscopic characterization of the NC samples. (*A*) Absorption and steady state PL spectra of 5 samples of CdSe/CdS/ZnS core/shell/shell NCs. (*B*) Typical time-resolved PL traces measured at 2 resolutions: 27.6 ps per channel for short time accuracy (*Left*) and 2.36 ns per channel width to capture the long PL tail (*Right*). Magnification reveals significant PL >2 μs after the excitation pulse. The short- and long-resolution data are fit simultaneously by using a multiexponential decay function (red lines). Residuals, shown at the top, attest to the accuracy of this procedure. Each of the decays is normalized between 1 (dark count) and 1,000. (*C*) The temperature dependence of average PL lifetimes, τ_{avg}, in these NCs is dominated by 2 lifetime regimes, identified by red and blue stripes. An initial (blue) drop in τ_{avg} in the smaller NCs is due to the lowest state in the exciton manifold, which is optically inert (dark). Subsequent undulations of τ_{avg} (red) are caused by a complex interplay between an activated trapping/detrapping process and the density of accessible trap states.

Results and Discussion

We selected 5 CdSe/CdS/ZnS NC samples with core diameters varying from 2.1 nm to 4.2 nm. Their absorption and steady-state PL spectra, plotted in Fig. 1*A*, show well resolved exciton absorption bands and narrow PL peaks with no trap emission. Well passivated core/shell NCs were investigated rather than, say, core-only samples, because they have fewer surface traps accessible to the exciton, and therefore provide clearer model systems. Time-resolved PL decays were measured at 12 temperatures from 77 K to 300 K and multiexponential decay functions were extracted by using a fitting procedure discussed in *Materials and Methods*. Typical PL transients are presented in Fig. 1*B*. The PL decays are multiexponential, which indicates the existence of a distribution of nonradiative transition frequencies. Notably, the tail of the decay stretches >2 μs beyond the initial excitation pulse. Multiexponential decay functions were extracted from these decays at each temperature, and average PL lifetimes, τ_{avg}, were calculated in the usual way (40). They are plotted versus temperature in Fig. 1*C*. The τ_{avg} parameter provides a way to monitor the general trends in the evolution of PL dynamics with temperature. Our data reveal a strong dependence of the dynamics on both temperature and NC diameter. Significantly, the data exhibit shared characteristics from one NC size to the next that suggest generalities in exciton–trap state interactions.

Two lifetime regimes are identified in Fig. 1*C*. The first (blue) regime dominates the low-temperature dynamics of the smaller NCs. It is consistent with previously observed (41) low-temperature CdSe PL measurements and is caused by the splitting of dark and bright exciton fine structure states in wurtzite NCs. Population in the lowest exciton state, which is dark, decreases with rising temperature and PL rates concomitantly quicken as the Boltzmann population of bright states increases. Because the bright–dark splitting is greatest in small NCs, this effect is largest in the 2 samples labeled I and II. The bright–dark splitting masks the observation of low-temperature trapping processes, so for our purposes it was unnecessary to measure PL decays <77 K.

The second regime, highlighted in red in Fig. 1*C*, arises as effects due to carrier trapping begin to dominate over purely excitonic processes. An initial rise of τ_{avg} with temperature in all of the samples is indicative of a growing trap state population and, hence, of an activated trapping process. At higher temperatures in the larger NCs, labeled III, IV, and V, τ_{avg} shows complex trends owing to interplay between trapping rates, detrapping rates, and the trap state distribution. A detailed analysis of these processes is beyond the scope of this article.

We emphasize 2 points drawn from the PL data presented in Fig. 1. First, the temperature dependence of the τ_{avg} data reveals that carrier detrapping on the timescales measured in our PL experiments occurs over an activation barrier rather than via temperature-independent quantum mechanical tunneling. Second, the multiexponential and long-lived nature of NC PL points to a distribution of activation barriers for the (de-)trapping reactions and indicates an energetic and/or spatial distribution of trap sites in and around the NCs. These 2 points form the foundation for our model of NC excitation dynamics.

Carrier trapping in nanocrystals converts a highly delocalized exciton state into a trap state in which one charge carrier is chiefly localized at the surface or at another interface. Significantly, we recognize that this process (whether it is electron or hole trapping) is an electron transfer (ET) reaction, which may be cast in terms of classical Marcus theory (42). To accomplish this requires a consideration of the factors that determine the nature of photoinduced ET reactions. With each transition, from an exciton state to a trap state, are associated 3 parameters: the free-energy difference, ΔG, between reactant and product; the reorganization energy, λ, that

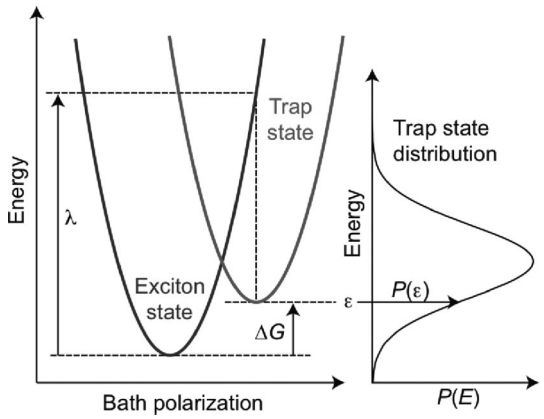

Fig. 2. A schematic ET framework to describe exciton dissociation/recombination processes. The right-hand parabola represents a trap state at energy, ε, which has a probability, $P(\varepsilon)$, of existing on a NC in the ensemble. The reorganization energy, λ, and free-energy change ΔG, of trapping and detrapping are defined relative to the exciton state.

enables the environment to accommodate the change in the charge distribution; and the electronic coupling integral between donor and acceptor states. This picture of trap state formation fundamentally distinguishes this work from previous studies on NC PL dynamics, because it encompasses effects due to both the nature of the NCs and, via ΔG and λ, the surrounding media. In this way our treatment provides a means to explicitly relate the properties of the local environment to their effect on NC PL dynamics.

Many accessible trap sites are likely to exist on a single NC, each with a discrete energy. In an ensemble of colloidal NCs, however, there is effectively a continuous distribution of trap state energies. If we assume that traps exist predominantly in narrow radial bands at NC interfaces such as the surface, spherical symmetry enables us to assume all interactions with traps at a particular interface are identical. We can then assign a single reorganization energy and electronic coupling parameter to all transitions between excitons and traps in each radial "trap-shell." In addition, the energies of trap states within each trap-shell in an ensemble of NCs can be approximated by a probability distribution. A schematic picture of the ET trapping model is shown in Fig. 2 and the mathematical details of the model are presented in supporting information (SI); they are not necessary to understand the results presented here. The model accounts for all 8 exciton fine structure states within the lowest manifold in addition to an arbitrary number of trap state distributions. Although higher energy exciton states may play a role in hot electron transfer, their contribution to the dynamics after the first few picoseconds is negligible due to tiny Boltzmann populations at these energies. Analysis of time-resolved PL data were facilitated by construction of a kinetic scheme based on the framework in Fig. 2. This was done in the manner discussed in detail by Jones *et al.* (43) with the assumption that nonradiative relaxation to the ground state can be neglected to simplify the analysis. This is justified by high PL quantum efficiencies (0.4–0.6 for each of the samples) and the fact that a proportion of the NCs are likely dark, as discussed below in relation to PL intermittency.

To reproduce a complex system, a realistic model must necessarily be complicated. Such a model, however, provides a powerful fitting function and care must be taken to ensure that extracted parameters reflect what is actually happening. We emphasize that our analyses were performed on a large quantity of data. To extract ET parameters for each NC sample, the combined data from 24 independently collected PL decay measurements, each collected over a substantial time range, were simultaneously analyzed. In addition, the electron transfer parameters obtained for each of our 5 NC samples are remarkably similar, reflecting perhaps the independence of trap states on NC size. However, the exchange parameter, used to describe exciton fine structure, was found to decrease with increasing NC size, as expected from theory (1). All parameters are tabulated in SI.

Application of our kinetic scheme to model PL decay functions is demonstrated in Fig. 3. Global analysis with a single kinetic scheme results in excellent reproduction of the decay functions at 12 temperatures. A minimum of 2 trap distributions, henceforth labeled K_1 and K_2, were necessary to yield an accurate reproduction of the PL dynamics in each of the 5 NC samples. The 2 trap distributions are quite distinct: transitions to K_1 are associated with large reorganization energies of ≈200 meV, whereas transitions to K_2 have much smaller values, ≈30 meV.

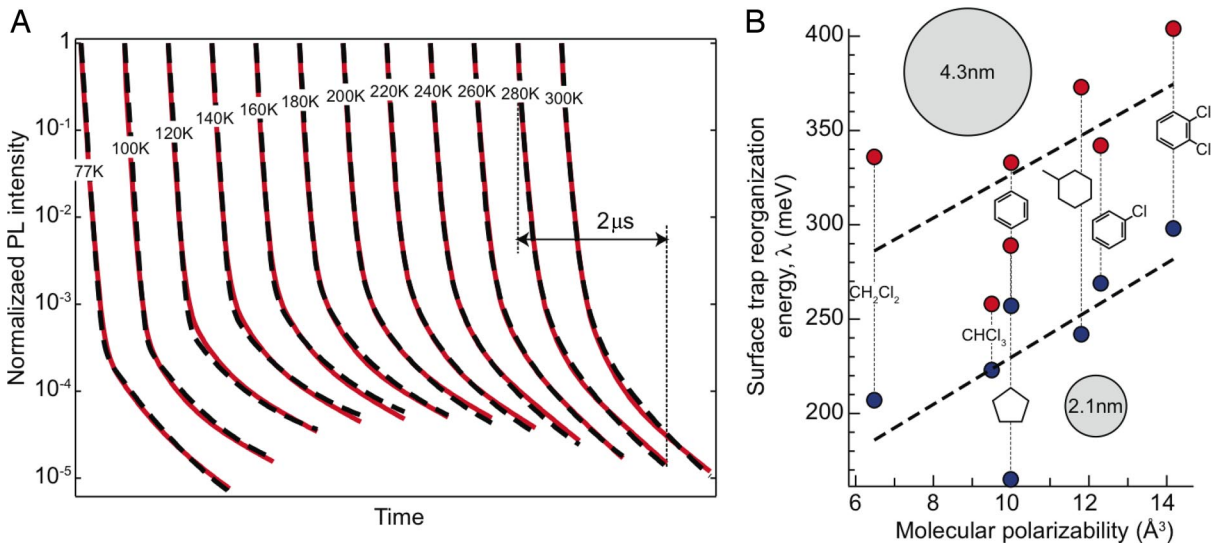

Fig. 3. Data analysis using the electron transfer scheme. (*A*) Global analysis of 12 PL decay functions (red lines) using a kinetic scheme with 2 trap-state distributions (black dashed lines). The decay functions were derived from multiexponential fits to single photon-counting data (e.g.: Fig. 1*B*) recorded from 77 to 300 K. Similarly excellent reproduction of decay functions was achieved for each of the 5 samples, often capturing >5 orders of magnitude of PL dynamics. (*B*) Reorganization energy of electron transfer between core and surface in small (blue circles) and large (red circles) NC samples (I and V in Fig. 1) is linearly correlated with the molecular polarizability of 7 solvents in which the NCs were dispersed. The dashed lines are linear fits to the data.

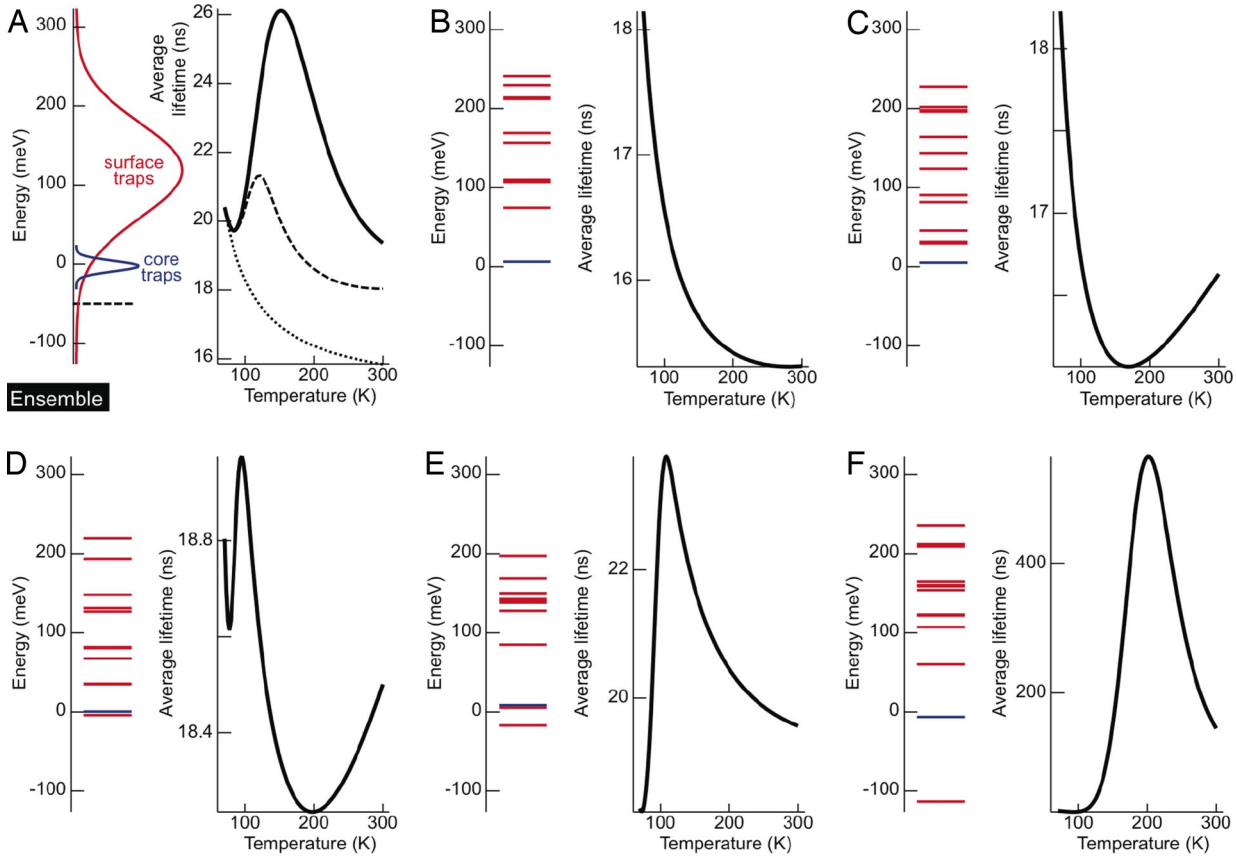

Fig. 4. Trap-state distributions and average PL lifetimes (thick black lines) for sample III (Fig. 1) calculated for the ensemble (*A*) and 5 selected individual NCs (*B–F*). Red lines denote surface traps and core/shell interface traps are blue. The energy scale is relative to the average energy of states in the ground exciton manifold. Depicted in *A* are ensemble average lifetimes computed respectively with all surface traps (dotted line) and all traps below −50 meV (dashed line) removed.

In addition, the peak of the K_1 and K_2 distributions lie at ≈130 meV and ≈5 meV above the exciton states, respectively. These values were found to be common to all 5 NC samples. A full list of trap state parameters is given in SI.

Large reorganization energies indicate that K_1 is likely to constitute a distribution of electron or hole traps on the NC surface. Charge transfer from a core exciton to surface traps that are close to mobile solvent and ligand molecules will likely involve significant nuclear reorganization, especially within the bath. It is unknown whether there would also be some local surface reconstruction in response to the trapped charge. Surface trap sites are located on the outermost ZnS shell, so trap state energies would be distributed on average higher than the CdSe exciton state, as is observed. Conversely, the K_2 trap parameters indicate that these could be interfacial trap sites near to the CdSe core. In this case electron transfer is likely to involve minimal nuclear reorganization within the lattice and the energy of these states is expected to be close to the exciton states. We find that the K_2 distribution is approximately Gaussian and spans a narrow energy range ($\sigma < 5$ meV), whereas the K_1 distribution is much broader ($25 < \sigma < 50$ meV) with a low-energy tail that extends below the energy of the exciton states.

Testing the predictions made by our model is an important step in showing it is consistent with the data. To do this we compared PL dynamics in a variety of solvents and examined the reorganization energy changes for photoinduced electron transfer reactions to our proposed K_1 surface traps. Seven additional noncoordinating solvents were selected, into which the smallest and largest NC samples (I and V in Fig. 1) were dispersed. Room temperature PL decays were measured and analyzed as before. Only reorganization energies were allowed to vary from the original parameter sets. The results, shown in Fig. 3*B*, represent a compelling argument for our electron transfer framework. We find a strong linear correlation between the reorganization energy for surface trapping and the molecular polarizability of the solvent. Given the magnitude of the correlation (≈100 meV from dichloromethane to *ortho*-dichlorobenzene) we can conclude that the outer-sphere or solvent component constitutes the main portion of the reorganization energy for exciton–surface electron transfer reactions.

In a related effect, single NCs examined under continuous photoexcitation show a blinking behavior whereby their PL switches on and off for periods that follow a power-law probability distribution and regularly exceeds 1 s (44). A distribution of long-lived dark states has been postulated as a cause for this effect (45). A key question about this process is its temperature independence between 10 K and 400 K (46, 47). By elucidating the basic photophysics of NCs we hope to illuminate the discussion of blinking with a more detailed understanding of trap properties.

Ensemble NC PL dynamics were accurately reproduced by using our ET framework, so we now consider predictions of the model at the single NC level. We modeled the trap states in the NC ensemble as the 2 distributions K_1 and K_2. At the level of a single NC in the ensemble those distributions determine the probability that a trap state of any particular energy will be found. The average numbers of trap states within each of the 2 distributions on a single NC are parameters in the ensemble-fitting process, and according to our fitting they are 13.1 and 1.2 for K_1 and K_2, respectively, in the CdSe/CdS/ZnS NCs in toluene solvent. By using a Monte Carlo approach, trap energies were chosen at random from the 2 ensem-

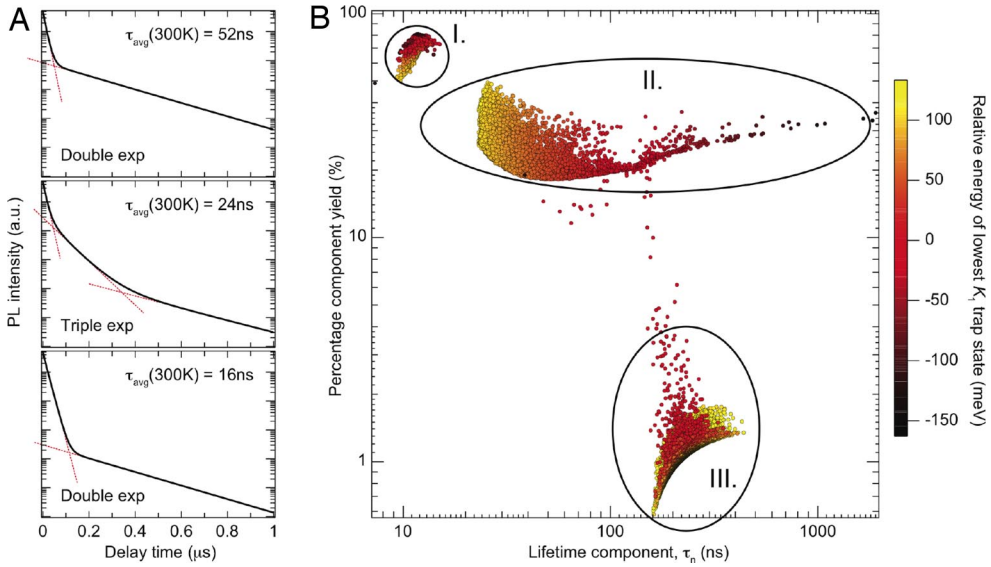

Fig. 5. Single NC PL dynamics. (*A*) Three representative short, medium, and long single-dot PL decays showing either bi- or triexponential decay kinetics. (*B*) Lifetime components extracted from 25,000 calculated single NC PL decays and plotted versus their relative contribution to the total PL signal. Markers are colored to indicate the position of the lowest-energy trap state relative to the average exciton energy.

ble distributions and single NC τ_{avg} values were calculated. Focusing on sample III from Fig. 1, we plot trap distribution energies and τ_{avg} versus temperature for the ensemble in Fig. 4*A* and for 5 selected single NCs in Fig. 4 *B–F*.

Strikingly, the calculated single NC τ_{avg} curves do not qualitatively resemble the ensemble data (from calculations or experiment), except in the few cases where one or more of the surface trap states has an energy (ε) lower than the ground state exciton manifold; however, this occurs infrequently because the probability distribution function of the surface traps is small when $\varepsilon < 0$. Average PL lifetime magnitudes are also smaller than the ensemble unless low-energy traps are present, indicating that contributions to the ensemble average PL lifetimes are strongly weighted by a small proportion of NCs with low-energy traps and very long τ_{avg} values, as in Fig. 4*F*. The significance of the $\varepsilon = 0$ crossing point can be understood when we consider (de-)trapping rates: below this energy the detrapping activation barrier (electron-hole recombination) becomes larger than the trapping barrier and the recombination rate becomes exponentially smaller than the trapping rate as the energy of the state drops further below the exciton. This is why trapped charges can be isolated on the surface for hundreds of nanoseconds or longer.

This observation indicates that the ensemble PL dynamics is especially sensitive to the existence of low-energy trap states. If we were to add more surfactant to sample III it is possible that some trap states would be removed by ligand passivation. To examine this we illustrate, in Fig. 4*A*, the predicted effect on the average lifetime curves for 2 cases: first, after removal of all of the surface states with energies >50 meV below the average exciton energy (amounting to only 0.001% of all K_1 traps); and second, after removal of all surface traps. The results demonstrate that removal of a tiny proportion of low-energy traps can induce a dramatic change in τ_{avg}, which explains why time-resolved NC PL is especially sensitive to slight environmental changes. Sensitivity of PL to low-energy traps is further demonstrated when we look closely at the ensemble PL signals at long times after photoexcitation. We calculate that 1 μs after photoexcitation of sample III at room temperature, 20% of the PL is produced by just 0.24% of the NCs.

These observations are relevant to considerations of the NC blinking effect mentioned earlier. Our analysis shows that NCs with very-low-energy trap states ($\varepsilon < -50$ meV) are rare, yet several of the models that account for single NC PL intermittency require the presence of deeply trapped states (45). Models including spectral diffusion of acceptor energies (46, 48) have previously been used to explain power-law blinking statistics. However, we find that trap energies in our samples are typically higher energy than would be required for blinking. It is possible that trap state distributions differ markedly between host environments, or that they change during the course of single NC measurements, sampling a wide range of energies within the ensemble distribution. Such processes would be caused by ligand desorption–adsorption equilibrium, which has been shown in PL and NMR studies to occur at timescales of a few seconds (49, 50).

Single NC PL decays can enable us to gain insight into ensemble trap distributions in the spirit of Fig. 4. Plotted in Fig. 5*A* are 3 representative calculated single NC PL decays. Those with short τ_{avg} and a very few with exceptionally long τ_{avg} are found to be biexponential, whereas, at intermediate times, the decays are triexponential. The short decay components in both bi- and triexponential decays remains fairly constant, but the 2 other components change markedly for different trap distributions. This is demonstrated in Fig. 5*B* in which decay components for 25,000 randomly generated single NCs have been calculated and are presented versus their percentage yield (the relative amount of PL that is emitted with that lifetime). We find that single NC decay components are almost entirely distributed within 3 regions in Fig. 5*B*, labeled I, II, and III. In addition, their positions within these distributions are strongly correlated in regions II and III with the energy of the lowest surface trap state. There is no correlation with region I because these components correspond to direct exciton recombination and are therefore little affected by trap energies. Because NCs with the lowest-energy traps produce PL decays with the longest lifetime components in region II, we assign this region to recombination of trapped carriers. Region III shows the reverse trend and is much weaker than region II, consistent with carrier trapping to a relatively small number of low-energy states. Fig. 5 provides a link with ensemble measurements: lifetime components extracted from an ensemble PL decay can be located on Fig. 5*B* and reveal the energy of the lowest NC trap states.

Conclusions

We have confirmed that electron or hole transfer to surface traps constitutes the dominant perturbative effect on the exciton dynam-

ics in core/shell CdSe NCs. Although the nature of these effects certainly depends on sample composition and condition, we have shown that they may be accessed from PL decays by using a chemically intuitive and general model. A major aim of work in this field is to be able to control the processes that occur between NC excitons and the surrounding environment. Trap states studied in our NC samples may be regarded as a model system for a wide range of reactions that transfer charge out of nanoscale materials and a deep understanding of these processes could potentially drive the application of NCs in photovoltaics (51, 52), sensors (53), or other applications that require the controlled interaction of nanoscale excitons.

Materials and Methods

CdSe core NCs overcoated with CdS then ZnS were provided by Evident Technologies. These were dispersed in a 6:1 mixture of isopentane and methylcyclohexane: a glass-forming solvent for low-temperature studies. The solutions were injected between 2 sapphire plates separated with a Teflon spacer and mounted on the sample holder. Other solvents used to disperse the NCs are indicated in the text. PL dynamics were measured by time-correlated single photon counting (TCSPC), using an IBH Datastation Hub system with an IBH 5000M PL monochromator and an R3809U-50 cooled MCP PMT detector. The light source was a model 3950 picosecond Ti:sapphire Tsunami laser (Spectra-Physics), pumped by a Millennium X (Spectra-Physics) diode laser and frequency doubled by using a GWU-23PL multiharmonic generator (Spectra-Physics). Sample temperatures were adjusted by using an N_2 flow cryostat coupled with a Lakeshore model 331 temperature controller.

Excitation wavelengths for the photon-counting experiments were set 400 meV higher energy than the peak of the room temperature absorption in each of the NC samples. Data were recorded for each sample at 77 K, 100 K, and then at 20 K intervals until 300 K. Emission wavelengths were adjusted, at each temperature, to remain coincident with the peak of the steady-state PL. To ensure that both the short- and long-decay components could be accurately extracted, PL decays were measured twice at each temperature: once with a 50-ns TAC ramp (27.6 ps channel width) and again with a 5-μs TAC (2.36-ns channel width).

Long and short TCSPC datasets were analyzed simultaneously by least-squares iterative reconvolution of an *N*-component multiexponential decay function with 2 experimentally determined instrument response functions (40). The value of *N* was determined, for each pair of datasets, as the minimum required to yield a satisfactory reproduction of the measured decay curves. Criteria for an acceptable fit have been justified in a previous article (43).

ACKNOWLEDGMENTS. This work was supported by The Natural Sciences and Engineering Research Council of Canada and by an E.W.R. Steacie Memorial Fellowship (to G.D.S.).

1. Scholes GD, Rumbles G (2006) Excitons in nanoscale systems. *Nat Mater* 5:683–696.
2. Huynh WU, Dittmer JJ, Alivisatos AP (2002) Hybrid nanorod-polymer solar cells. *Science* 295:2425–2427.
3. Bryant GW, Jaskolski W (2005) Surface effects on capped and uncapped nanocrystals. *J Phys Chem B* 109:19650–19656.
4. Dayal S, Burda C (2007) Surface effects on quantum dot-based energy transfer. *J Am Chem Soc* 129:7977–7981.
5. Smith AM, Duan HW, Rhyner MN, Ruan G, Nie SM (2006) A systematic examination of surface coatings on the optical and chemical properties of semiconductor quantum dots. *Phys Chem Chem Phys* 8:3895–3903.
6. Qu LH, Peng XG (2002) Control of photoluminescence properties of CdSe nanocrystals in growth. *J Am Chem Soc* 124:2049–2055.
7. Xie RG, Kolb U, Li JB, Basche T, Mews A (2005) Synthesis and characterization of highly luminescent CdSe-Core CdS/Zn0.5Cd0.5S/ZnS multishell nanocrystals. *J Am Chem Soc* 127:7480–7488.
8. Talapin DV, Rogach AL, Kornowski A, Haase M, Weller H (2001) Highly luminescent monodisperse CdSe and CdSe/ZnS nanocrystals synthesized in a hexadecylamine-trioctylphosphine oxide-trioctylphospine mixture. *Nano Lett* 1:207–211.
9. Kalyuzhny G, Murray R (2005) Ligand effects on optical properties of CdSe nanocrystals. *J Phys Chem B* 109:7012–7021.
10. Underwood DF, Kippeny T, Rosenthal SJ (2001) Ultrafast carrier dynamics in CdSe nanocrystals determined by femtosecond fluorescence upconversion spectroscopy. *J Phys Chem B* 105:436–443.
11. Creti A, *et al.* (2006) Role of the shell thickness in stimulated emission and photoinduced absorption in CdSe core/shell nanorods. *Phys Rev B* 73:165410.
12. Califano M, Franceschetti A, Zunger A (2005) Temperature dependence of excitonic radiative decay in CdSe quantum dots: The role of surface hole traps. *Nano Lett* 5:2360–2364.
13. Bawendi MG, Steigerwald ML, Brus LE (1990) The quantum-mechanics of larger semiconductor clusters (quantum dots). *Annu Rev Phys Chem* 41:477–496.
14. Alivisatos AP (1996) Perspectives on the physical chemistry of semiconductor nanocrystals. *J Phys Chem* 100:13226–13239.
15. Klimov VI, *et al.* (2000) Optical gain and stimulated emission in nanocrystal quantum dots. *Science* 290:314–317.
16. El-Sayed M (2004) Small is different: Shape-, size-, and composition-dependent properties of some colloidal semiconductor nanocrystals. *Acc Chem Res* 37:326–333.
17. Scholes GD (2008) Controlling the optical properties of inorganic nanoparticles. *Adv Funct Mater* 18:1157–1172.
18. Ratcliffe CI, *et al.* (2006) Solid state NMR studies of photoluminescent cadmium chalcogenide nanoparticles. *Phys Chem Chem Phys* 8:3510–3519.
19. Berrettini MG, Braun G, Hu JG, Strouse GF (2004) NMR analysis of surfaces and interfaces in 2-nm CdSe. *J Am Chem Soc* 126:7063–7070.
20. Majetich SA, Carter AC, Belot JA, McCullough RD (1994) H1 NMR characterization of the CdSe nanocrystallite surface. *J Phys Chem* 98:13705–13710.
21. Wang W, Banerjee S, Jia SG, Steigerwald ML, Herman IP (2007) Ligand control of growth, morphology, and capping structure of colloidal CdSe nanorods. *Chem Mater* 19:2573–2580.
22. Liu HT, Owen JS, Alivisatos AP (2007) Mechanistic study of precursor evolution in colloidal group II-VI semiconductor nanocrystal synthesis. *J Am Chem Soc* 129:305–312.
23. Micic OI, *et al.* (2002) Electron and hole adducts formed in illuminated InP colloidal quantum dots studied by electron paramagnetic resonance. *J Phys Chem B* 106:4390–4395.
24. Eijt SWH, *et al.* (2006) Study of colloidal quantum-dot surfaces using an innovative thin-film positron 2D-ACAR method. *Nat Mater* 5:23–26.
25. Carter AC, *et al.* (1997) Surface structure of cadmium selenide nanocrystallites. *Phys Rev B* 55:13822–13828.
26. Zhang HZ, Gilbert B, Huang F, Banfield JF (2003) Water-driven structure transformation in nanoparticles at room temperature. *Nature* 424:1025–1029.
27. Puzder A, Williamson AJ, Gygi F, Galli G (2004) Self-healing of CdSe nanocrystals: First-principles calculations. *Phys Rev Lett* 92:217401.
28. Krauss TD, O'Brien S, Brus L (2001) Charge and photoionization properties of single semiconductor nanocrystals. *J Phys Chem B* 105:1725–1733.
29. Lifshitz E, Dag I, Litvitn ID, Hodes G (1998) Optically detected magnetic resonance study of electron/hole traps on CdSe quantum dot surfaces. *J Phys Chem B* 102:9245–9250.
30. Lifshitz E, Glozman A, Litvin ID, Porteanu H (2000) Optically detected magnetic resonance studies of the surface/interface properties of II–VI semiconductor quantum dots. *J Phys Chem B* 104:10449–10461.
31. Hong M, Guo-Hong M, Wen-Jun W, Xue-Xi G, Hong-Liang M (2008) Size-dependent optical properties and carriers dynamics in CdSe/ZnS quantum dots. *Chinese Phys B* 17:1280–1285.
32. Morello G, *et al.* (2007) Picosecond photoluminescence decay time in colloidal nanocrystals: The role of intrinsic and surface states. *J Phys Chem C* 111:10541–10545.
33. Lee WZ, *et al.* (2005) Recombination dynamics of luminescence in colloidal CdSe/ZrS quantum dots. *Nanotechnology* 16:1517–1521.
34. Wuister SF, Donega CD, Meijerink A (2004) Local-field effects on the spontaneous emission rate of CdTe and CdSe quantum dots in dielectric media. *J Chem Phys* 121:4310–4315.
35. Wuister SF, van Houselt A, Donega CD, Vanmaekelbergh D, Meijerink A (2004) Temperature antiquenching of the luminescence from capped CdSe quantum dots. *Angew Chem Int Ed* 43:3029–3033.
36. Wang XY, Qu LH, Zhang JY, Peng XG, Xiao M (2003) Surface-related emission in highly luminescent CdSe quantum dots. *Nano Lett* 3:1103–1106.
37. Fisher BR, Eisler HJ, Stott NE, Bawendi MG (2004) Emission intensity dependence and single-exponential behavior in single colloidal quantum dot fluorescence lifetimes. *J Phys Chem B* 108:143–148.
38. Jones M, Nedeljkovic J, Ellingson RJ, Nozik AJ, Rumbles G (2003) Photoenhancement of luminescence in colloidal CdSe quantum dot solutions. *J Phys Chem B* 107:11346–11352.
39. Crooker SA, Barrick T, Hollingsworth JA, Klimov VI (2003) Multiple temperature regimes of radiative decay in CdSe nanocrystal quantum dots: Intrinsic limits to the dark-exciton lifetime. *Appl Phys Lett* 82:2793–2795.
40. O'Connor DV, Phillips D (1984) *Time-Correlated Single Photon Counting* (Academic, London).
41. Donega CdM, Bode M, Meijerink A (2006) Size- and temperature-dependence of exciton lifetimes in CdSe quantum dots. *Phys Rev B* 74:1–9.
42. Marcus RA, Sutin N (1985) Electron transfers in chemistry and biology. *Biochim Biophys Acta* 811:265–322.
43. Jones M, Kumar S, Lo SS, Scholes GD (2008) Exciton trapping and recombination in type IICdSe/CdTe nanorod heterostructures. *J Phys Chem C* 112:5423–5431.
44. Nirmal M, *et al.* (1996) Fluorescence intermittency in single cadmium selenide nanocrystals. *Nature* 383:802–804.
45. Frantsuzov P, Kuno M, Janko B, Marcus RA (2008) Universal emission intermittency in quantum dots, nanorods and nanowires. *Nat Phys* 4:519–522.
46. Shimizu KT, *et al.* (2001) Blinking statistics in single semiconductor nanocrystal quantum dots. *Phys Rev B* 63:205316.
47. Kuno M, Fromm DP, Hamann HF, Gallagher A, Nesbitt DJ (2001) ''On''/''off'' fluorescence intermittency of single semiconductor quantum dots. *J Chem Phys* 115:1028–1040.
48. Pelton M, Smith G, Scherer NF, Marcus RA (2007) Evidence for a diffusion-controlled mechanism for fluorescence blinking of colloidal quantum dots. *Proc Natl Acad Sci USA* 104:14249–14254.
49. Bullen C, Mulvaney P (2006) The effects of chemisorption on the luminescence of CdSe quantum dots. *Langmuir* 22:3007–3013.
50. Ji X, Copenhaver D, Sichmeller C, Peng X (2008) Ligand bonding and dynamics on colloidal nanocrystals at room temperature: The case of alkylamines on CdSe nanocrystals. *J Am Chem Soc* 130:5726–5735.
51. Gur I, Fromer NA, Geier ML, Alivisatos AP (2005) Air-stable all-inorganic nanocrystal solar cells processed from solution. *Science* 310:462–465.
52. Nozik, A. J. (2002) Quantum dot solar cells. *Physica E* 14:115–120.
53. Heafey E, Laferriere M, Scaiano JC (2007) Comparative study of the quenching of core and core-shell CdSe quantum dots by binding and non-binding nitroxides. *Photochem Photobiol Sci* 6:580–584.